Food Hydrocolloids 25 (2011) 1–11

Contents lists available at ScienceDirect

Food Hydrocolloids

journal homepage: www.elsevier.com/locate/foodhyd

Hydroxypropylmethylcellulose at the oil–water interface. Part I. Bulk behaviour and dynamic adsorption as affected by pH

Nerina A. Camino [a], Cecilio Carrera Sánchez [b], Juan M. Rodríguez Patino [b], Ana M.R. Pilosof [a,*]

[a] CONICET, Departamento de Industrias, Facultad de Ciencias Exactas y Naturales, Ciudad Universitaria, Universidad de Buenos Aires, Intendente Guiraldes s/n, 1428 Buenos Aires, Argentina

[b] Departamento de Ingeniería Química, Facultad de Química, c/o Prof. García González, Universidad de Sevilla, 41012 Seville, Spain

ARTICLE INFO

Article history:
Received 19 November 2009
Accepted 25 April 2010

Keywords:
Hydroxypropylmethylcellulose
Adsorption
Oil–water interface
Hydrophobic interactions

ABSTRACT

The bulk and oil–water (O/W) surface behaviour of four different commercial types of hydroxypropylmethylcelluloses (HPMCs) was studied at pH3 and 6.

Dynamic light scattering (DLS) analysis of particle size distribution in HPMC water solutions indicated cluster formation at pH6 for most types.

The dynamics of adsorption showed that the surface pressure (π) values and the rate of adsorption/penetration were lower at pH3.

The surface dilatational modulus of films at pH6 showed a continuous increase indicating a slow formation of a viscoelastic interfacial film. Nevertheless, at pH3 in most cases a viscoelastic film was not formed.

The results obtained at the oil–water interface well correlated with DLS.

Among all the HPMC studied, E5LV showed over all the best performance at this oil–water interface due to its low molecular weight and high decrease of interfacial tension. Its high hydrophobicity allows a strong tendency to interact at the interface to form elastic films.

1. Introduction

Many natural and processed foods consist either partly or wholly as emulsions or have been in an emulsified state at some time during their production (McClements, 1999).

Emulsions are thermodynamically unstable systems because of unfavourable contact between oil and water phases, and because the oil and water phases have different densities, they will always breakdown over time (Moreau, Kim, Decker, & McClements, 2003).

The interfacial region which separates the oil from the aqueous phase constitutes only a small fraction of the total volume of an emulsion. Nevertheless, it has a direct influence on the bulk physicochemical and sensory properties of food emulsions, including their formation, stability, rheology and flavour (McClements, 1999).

Emulsions breakdown is usually retarded by using emulsifiers, which are surface-active ingredients that adsorb to the surface of freshly formed oil droplets during homogenization. Once adsorbed they facilitate further droplet disruption by lowering the interfacial tension, thereby reducing the size of the droplets produced during homogenization. Emulsifiers also reduce the tendency for droplets to aggregate by forming protective films and/or generating repulsive forces between the droplets. A good emulsifier should rapidly adsorb at the surface of oil droplets formed during homogenization, rapidly lower the interfacial tension by a significant amount and protect the droplets against aggregation during emulsions processing, storage, and utilization (McClements, 1999; Moreau et al., 2003).

Moreover, good thickening ability, the formation of an elastic gel-like film and the protective colloid effect by adsorption at the oil–water interface are responsible for the stability of oil-in-water emulsions stabilized by biopolymers (Akiyama et al., 2005).

Sun, Sun, Wei, Liu, and Zhang (2007) stayed that the stability of emulsions prepared with hydrophobically modified hydroxyethyl cellulose (HMHEC) is based on both an associative thickening mechanism caused by alkyl chains in HMHEC and the adsorption of HMHEC at the oil–water interface, which can form a solid film preventing coalescence of the droplets. Mezdour, Lepine, Erazo-Majewicz, Ducept, and Michon (2008) studying hydroxypropylcellulose (HPC) adsorption at the oil–water interface, found that the surface tension lowering and the rheological properties of the polymer layer formed at the interface appear to be key factors affecting the stability of the emulsions.

* Corresponding author. Tel.: +54 11 4576 3377; fax: +54 11 4576 3366.
E-mail address: apilosof@di.fcen.uba.ar (A.M.R. Pilosof).

0268-005X/$ – see front matter © 2010 Elsevier Ltd. All rights reserved.
doi:10.1016/j.foodhyd.2010.04.012

Perrin and Lafuma (1998) pointed out that emulsions properties were closely dependent on molecular weight and hydrophobic modification of hydrophobically grafted poly(sodium acrylates) as well as on emulsifier concentration, and all the factors led to variation of the viscosity of the aqueous polymer solutions.

A wide variety of different kinds of synthetic and natural emulsifiers can be used in food emulsions, including small-molecule surfactants, phospholipids, proteins and polysaccharides (Moreau et al., 2003). Among the last group are the cellulose derivatives which have a strong tendency to accumulate at the air–water and the oil–water interface (Nahringbauer, 1995). Although, only four of them are used in the food area for their surface tension reducing properties: methylcellulose (MC), carboxymethylcellulose (CMC), hydroxypropylcellulose (HPC) and hydroxypropylmethylcellulose (HPMC). Even, ethylcellulose and hydroxypropylmethylcellulose appear to be more surface active than milk proteins (Arboleya & Wilde, 2005; Mezdour, Cuvelier, Cash, & Michon, 2007; Pérez, Carrera-Sánchez, Rodríguez-Patino, & Pilosof, 2007). The hydroxypropylmethylcelluloses (HPMCs) are polymers with methyl and hydroxypropyl groups added to the anhydroglucose backbone. They include a family of cellulose ethers that differ principally in molecular weight, viscosity, degree of substitution (DS), and molar substitution (MS) (Williams & Prins, 1996). To be precise, DS defines the average number of hydroxyl groups per anhydroglucose unit where hydrogen is replaced by methyl, and MS represents the average number of propylene oxide groups per anhydroglucose unit (Nahringbauer, 1995). Along the cellulose backbone, methyl substitutes constitute hydrophobic zones whereas hydroxypropyl groups are more hydrophilic. The introduction of these groups allows HPMC to behave as a surfactant. Thus HPMCs are adsorbed at fluid interfaces lowering the surface tension (Daniels & Barta, 1993; Daniels & Barta, 1994; Nahringbauer, 1995; Ochoa Machiste & Buckton, 1996; Wollenweber, Makievski, Miller, & Daniels, 2000).

HPMC is much more surface active than most proteins (Arboleya & Wilde, 2005; Mezdour et al., 2007; Pérez et al., 2007). It has been previously reported that HPMC dominates surface pressure in mixtures with proteins even when both components can saturate the interface (Martinez, Carrera Sanchez, Ruiz Henestrosa, Rodriguez Patino, & Pilosof, 2007; Pérez et al., 2007).

Few investigations have been reported on the polysaccharides dynamic adsorption at the oil–water interface in the literature. Thus, the objective of the present work was to study the dynamic surface behaviour of four commercial types of HPMCs at the O/W interface at pH3 and 6, at which HPMCs emulsions will be studied alone and in more complex systems, i.e. mixed with milk proteins, in a forthcoming research.

2. Materials and methods

2.1. Materials

Methocell E5LV, E15LV, E50LV and E4M (food grade) from the Dow Chemical Company were kindly supplied by Colorcon Argentina and used without purification. Table 1 shows some characteristic properties, such as methyl and hydroxypropyl content, methyl/hydroxypropyl ratio, molar substitution, the degree of substitution, the viscosity (20 °C) of 2%wt solutions, and molecular weight. The moisture content of HPMC powders was 1.6%.

HPMC solutions at 1×10^{-2}%wt, 1%wt and 2%wt, were prepared at 90 °C by dispersing the powder in buffer SÖrensen solutions, phosphate for pH6 or citrate/chlorine for pH3, and cooled down to room temperature. Milli-Q ultrapure water was used for buffer preparation. The pH and ionic strength ($I = 5$ mM) were kept constant. The solutions were stored at 4 °C for 24 h to achieve the maximum polysaccharide hydration.

Table 1
Properties of E4M, E50LV, E15LV and E5LV.

HPMC	E4M	E50LV	E15LV	E5LV
% Methyl	28.0	29.1	29.2	29.5
% Hydroxypropyl	10.2	9.2	9.3	9.7
Methyl/hydroxypropyl ratio	2.3	3.2	3.1	3.0
Methyl substitution (DS)	1.90	1.90	1.90	1.90
Hydroxypropyl substitution (MS)	0.23	0.23	0.23	0.23
Total substitution (DS + MS)	2.13	2.13	2.13	2.13
Viscosity (cp), 2%wt solution, 20 °C	4965	41	15	5.4
Molecular weight (Da)	90,000	18,000	6000	2000

The materials in contact with the solutions were properly cleaned in order to avoid any contamination by any surface-active substance. The absence of surface-active contaminants in the aqueous buffered solutions was checked by surface tension measurements before sample preparation. No aqueous solutions with a surface tension other than that accepted in the literature (72–73 mN/m at 20 °C) were used.

Commercial sunflower oil was used as the oil phase in this research without further purification in order to study the performance of HPMCs in a real interface (i.e. commercial oil widely used in food industry), the same to be used in emulsification studies.

In order to check differences in the interfacial behaviour of HPMCs that could be attributed to the heterogeneous composition of commercial oil, some adsorption measurements were performed using purified oil (Florisil 60–100 mesh Aldrich®). The commercial sunflower oil and Florisil were allowed to interact for 24 h and then filtered (0.22 μm) the upper phase free of impurities.

Sunflower oil contains triglycerides and both, saturated and unsaturated fatty acid. The alkyl chain lengths of these fatty acids vary between 14 and 22. Therefore, from surface science point of view, sunflower oil is a complex mixture (Wüstneck, Moser, & Muschiolik, 1999).

2.2. Dynamic interfacial properties

All the experiments in the automatic drop tensiometer, were carried out at 20 °C and the temperature of the system was maintained constant within ±0.1 °C by circulating water from a thermostat. The final concentrations of HPMC in the sub-phase were 1×10^{-2}%wt, 1%wt and 2%wt. The solutions were placed in the syringe and then in the compartment and were allowed to stand for 30 min to reach the desired constant temperature. Then a drop of HPMC solution was delivered to achieve macromolecule adsorption at the O/W interface, where the cell was filled with the oil while the syringe break the aqueous HPMCs solutions free into it.

The materials in contact with HPMC solutions were properly cleaned in order to avoid any contamination by any surface-active substance.

2.2.1. Dynamic interfacial tension

Time-dependent surface pressure of adsorbed HPMC films at the O/W interface was determined by an automatic drop tensiometer (IT Concept, France) as described elsewhere (Baeza, Carrera Sanchez, Pilosof, & Rodríguez Patino, 2005; Rodríguez Niño & Rodríguez Patino, 2002). The surface tension (γ) was calculated thorough the analysis of the droplet profile (Labourdenne et al., 1994). The surface pressure is $\pi = \gamma^{o} - \gamma$, where γ^{o} is the sub-phase interfacial tension (29.5 mN/m) and γ the interfacial tension of solution at each time (θ). The average accuracy of the interfacial tension is roughly 0.1 mN/m. However, the reproducibility of the results, for at least two measurements, was better than 1%.

From the adsorption dynamics measurements, the adsorption kinetic parameters can be obtained. The main features of the kinetics of adsorption of HPMC include (i) the diffusion of the protein from the bulk onto the interface, (ii) adsorption (penetration) and interfacial unfolding, and (iii) aggregation (rearrangement) within the interfacial layer, multilayer formation and even interfacial gelation (MacRitchie, 1990; Nahringbauer, 1995; Perez, Carrera Sanchez, Rodriguez Patino, & Pilosof, 2006; Pérez, Sánchez, Pilosof, & Rodríguez Patino, 2008; Wollenweber et al., 2000).

During the first step, at relatively low surface pressures when diffusion is the rate-determining step, a modified form of the Ward and Tordai equation can be used to correlate the change in surface pressure with time (Ward & Tordai, 1946):

$$\pi = 2C_0KT\left(D_{\text{diff}}\theta/3.14\right)^{1/2} \tag{1}$$

where C_o is the concentration in the aqueous phase, K the Boltzmann constant, T the absolute temperature, D_{diff} the diffusion coefficient, and θ the adsorption time. If the diffusion at the interface controls the adsorption process, a plot of π against $\theta^{1/2}$ will then be linear (de Feijter & Benjamins, 1987; MacRitchie, 1990; Pérez et al., 2008; Xu & Damodaran, 1994) and the slope of this plot will be the diffusion rate (K_{diff}).

To analyze the rate of adsorption (penetration) and rearrangement of adsorbed biopolymer the following phenomenological first-order equation, proposed by Graham and Phillips (1979), has been used:

$$\ln\left(\frac{\pi_{180}-\pi_\theta}{\pi_{180}-\pi_0}\right) = -k_i\cdot\theta \tag{2}$$

where π_{180}, π_0, and π_θ are the surface pressures at 180 min of adsorption time, at time $\theta = 0$, and at any time, θ, respectively, and k_i is the first-order rate.

2.2.2. Surface dilatational properties

The surface viscoelastic parameters (surface dilatational modulus, E, and its elastic, E_d, and viscous, E_v, components), were measured as a function of time, θ, at 10% deformation amplitude ($\Delta A/A$) and 0.1 Hz of angular frequency (ω). Previously, the percentage area change had been determined to be in the linear region (data not shown) for both pH. The method involved a periodic automated-controlled, sinusoidal interfacial compression and expansion performed by decreasing and increasing the drop volume, at the desired amplitude. The surface dilatational modulus derived from the change in surface tension (dilatational stress), σ (equation (3)), resulting from a small change in surface area (dilatational strain), A (equation (4)), may be described by equation (5) (Lucassen & van den Temple, 1972)

$$\sigma = \sigma_0\sin(\omega\theta+\delta) \tag{3}$$

$$A = A_0\sin(\omega\theta) \tag{4}$$

$$E = \frac{d\sigma}{dA/A} = -\frac{d\pi}{d\ln A} = E_d + iE_v \tag{5}$$

where σ_0 and A_0 are the stress and strain amplitudes, respectively, and δ is the phase angle between stress and strain.

The dilatational modulus is a complex quantity, which is composed of real and imaginary parts:

The real part of the dilatational modulus or storage component is the dilatational elasticity, $E_d = |E|\cos\delta$. The imaginary part of the dilatational modulus or loss component is the surface dilatational viscosity$E_v = |E|\sin\delta$. The modulus $|E|$ is a measure of the total unit material dilatational resistance to deformation (elastic + viscous). For a perfectly elastic material, the stress and strain are in phase ($\delta = 0$) and the imaginary term is zero. In the case of a perfectly viscous material $\delta = 90^\circ$ and the real part is zero. The loss angle tangent can be defined by equation (7). Thus, if the film is purely elastic, the loss angle tangent is zero.

$$\tan\delta = E_v/E_d \tag{7}$$

2.3. Dynamic light scattering measurements

Dynamic light scattering (DLS) experiments were carried out in a Dynamic Laser Light Scattering instrument (Zetasizer Nano-Zs, Malvern Instruments, Worcestershire, United Kingdom) provided with a He–Ne laser (633 nm) and a digital correlator, Model ZEN3600. Measurements were carried out at a fixed scattering angle of 173° and at 25 °C. Samples at 2%wt were contained in a disposable polystyrene cuvette. The average value and standard deviation of ten measurements per sample is reported.

In DLS, the sample is illuminated with a laser beam and the intensity of the resulting scattered light produced by the particles fluctuates at a rate that is dependent upon the size of the particles. Analysis of these intensity fluctuations yields the diffusion coefficient of the particle. The particle size is then calculated from the translational diffusion coefficient by using de Stokes–Einstein equation:

$$d_h = \frac{kT}{3\pi\eta D} \tag{8}$$

where, d_h is the hydrodynamic diameter; D the translational diffusion coefficient; k the Boltzmann's constant; T the absolute temperature and η the viscosity.

There are two approaches that can be utilized to obtain size information (i) Cumulant analysis fit a single exponential to the correlation function to obtain the mean size (z-average diameter) and an estimate of the width of the distribution (polydispersity index) know as a measure of the degree of aggregation (ii) CONTIN analysis fit a multiple exponential to the correlation function to obtain the percentile distribution of particle/aggregates sizes providing a plot of the relative intensity of light scattered by particles in various size classes (intensity size distribution). Through Mie theory, the original intensity distribution can be converted into volume and number distributions.

2.4. Zeta-potential measurements

Zeta-potential measurements (ξ) were carried out in a Dynamic Laser Light Scattering instrument (Zetasizer Nano-Zs, Malvern Instruments, Worcestershire, United Kingdom) provided with a He–Ne laser (633 nm) and a digital correlator, Model ZEN3600. Measurements were carried out at a fixed scattering angle of 17°. Samples at 2%wt were previously diluted 1:100 to a droplet concentration of 0.02%wt with the corresponding buffer solution and then contained in a measurements chamber of a particle electrophoresis instrument. The zeta-potential was determined by measuring the direction and velocity that the droplets moved in the applied electric field at 25 °C. The zeta-potential measurements are reported as the average and standard deviation of measurements made on two samples, with ten readings made per sample.

The Zetasizer Nano series calculates the zeta potential by determining the electrophoretic mobility and then applying the Henry equation. The electrophoretic mobility is obtained by performing an electrophoresis experiment on the sample and measuring the velocity of the particles using Laser Doppler Velocimetry (LDV).

Henry equation:

$$U_E = \frac{2\varepsilon z f(Ka)}{3\mu} \quad (9)$$

where

z is the zeta potential.
U_E is the electrophoretic mobility.
ε is the dielectric constant.
η is the viscosity.
and $f(Ka)$ is the Henry's function. Two values are generally used as approximations for the $f(Ka)$ determination either 1.5 or 1.0. In aqueous media and low electrolyte concentration, as in this work, the 1.0 value is used (Huckel approximation).

3. Results

3.1. Characterization of particle size distribution of HPMC solutions

HPMC polymers are polydispersed materials in terms of their chemical composition and molecular weight distribution, meaning that each polysaccharide contains chains of different numbers of monosaccharide units giving a distribution of molecular weight (Pérez, Carrera Sánchez, Pilosof, & Rodríguez Patino, 2009; Viriden, Wittgren, Andersson, & Larsson, 2009). The heterogeneous nature of cellulose leads to variations in the availability and reactivity of the hydroxyl groups. To decrease the variations between commercial HPMC grade used, the polymer samples must have average viscosities and average degree of substitution within certain limits, which are stated in the pharmacopeias (U.S.P., 2008). In the area of polymer chemistry, polydispersity can be measured experimentally by dynamic light scattering.

Table 1 shows some characteristic properties of the HPMC used in this research. All of them belong to the same family of HPMC (serie E), with the same degree of substitution close to 2, that accounts for a high degree of hydrophobicity, necessary for surface activity (Pérez et al., 2007). E4M posses the lowest % methyl substituent and the highest % hydroxypropyl substituent, which makes it the less hydrophobic HPMC, accounting for its lowest methyl/hydroxypropyl ratio (2.3). The other three HPMC studied, E5LV, E15LV and E50LV, have similar % substituents and methyl/hydroxypropyl ratio (3.0). E4M also has the higher molecular weight and viscosity.

Fig. 1 shows the volume size distribution for the HPMCs at 2% bulk concentration. At pH3 the distributions were bimodal with a predominant lower size peak at around 2, 4 and 6 nm for E5LV, E15LV and E50LV respectively. Only E4M solutions at pH3 presented a monomodal distribution with the maximum of the size peak at 10 nm.

A rough estimate of molecular weight of HPMCs made with the software of the Zetasizer Nano-Zs instrument, for linear polysaccharides, indicates that these values correspond to 2.1, 7.4, 15 and 39 kDa for E5LV, E15LV, E50LV and E4M respectively. Nevertheless, the predominant peaks were broad, being the width indicative of the existence of molecular weight distribution. The estimate molecular weight ranges on the basis of the width of the peak were 0.9–7.7 kDa for E5LV; 2.7–12 kDa for E15LV; 4.6–40 kDa for E50LV and 10.1–246.8 kDa for E4M. As can be deduced, the average molecular weight reported in Table 1 for the monomers, fall within the observed molecular weight distribution range for each HPMC. The lower volume peak observed at pH3 (Fig. 1) corresponds to aggregates or clusters formed by all HPMCs. The higher tendency to cluster formation of E5LV, E15LV and E50LV would be ascribed to the higher methyl substitution which allows stronger hydrophobic interactions. It has been reported that polysaccharides tend to form larger aggregates in the aqueous media with increasing its molecular weight and/or concentration (Camino, Perez, & Pilosof, 2009; Doublier & Launay, 1981; Kato, Yokoyama, & Takahashi, 1978).

At pH6 all the distributions were monomodal, with a broad peak indicating the existence of broad particle size distribution. This peak (except for E4M), mainly coincided with the minor peak

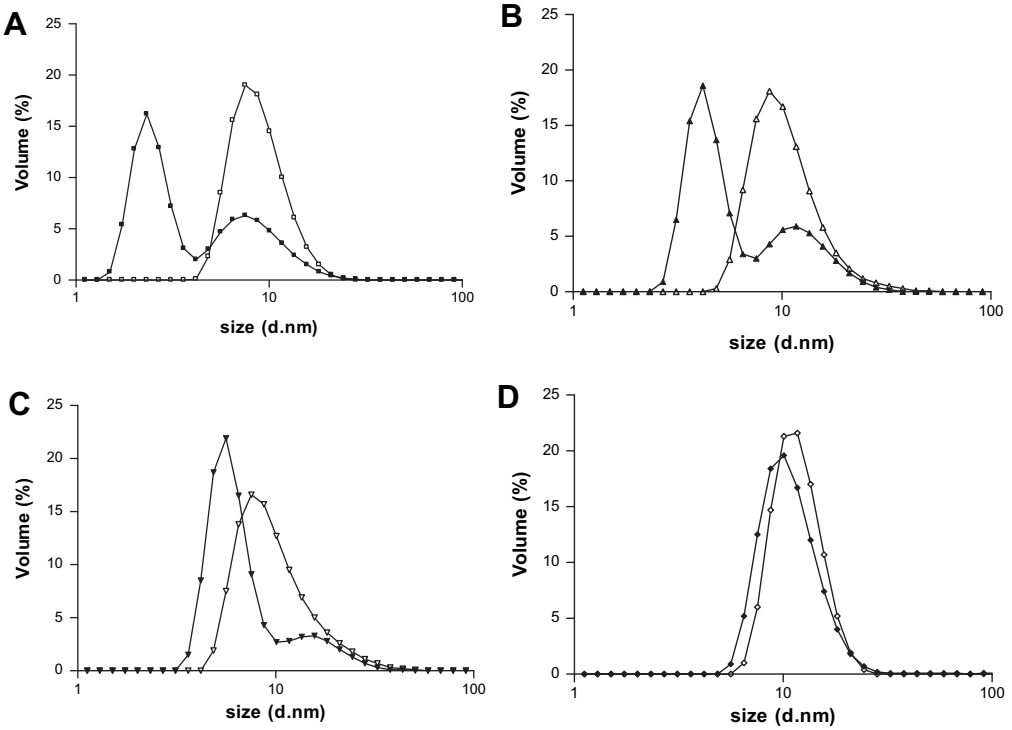

Fig. 1. Volume particle size distribution of HPMC 2%wt solutions at pH3 (full symbols) and pH6 (empty symbols) for E5LV (A), E15LV (B), E50LV (C) and E4M (D).

observed at pH3 around 10 nm, attributed to cluster formation. It can also be observed the absence of a peak at lower sizes as observed at pH3. The maximum of the monomodal peak was around 8 nm for E5LV, E15LV and E50LV indicating the absence of monomeric forms. E4M was slightly affected by pH (Fig. 1D), the cluster formation were higher at pH6. This behaviour would be related with the lower tendency to association at higher polysaccharide molecular weight (Sarkar, 1977) and to the lowest percentage of methyl groups (Table 1).

At pH3, HPMCs present a small negative net superficial charge determined by zeta-potential measurements (Table 2) but at pH6 the zeta potential became slightly positive (Table 2), which seems to be correlated to the strong tendency to cluster formation observed in Fig. 1.

Nevertheless, the zeta-potential magnitude (negative charge) is not higher enough to explain the lower methyl interaction due to electrostatic repulsion at pH3.

At low temperatures, the water molecules are situated around the methyl groups in *cage-like* structures (Sarkar & Walker, 1995).It could be possible that the chloride ions of the buffer were interacting with the cage-like structures and, therefore, impeding the cluster formation.

3.2. Dynamics of HPMCs adsorption at the oil–water interface

First of all, to establish the contribution of the oil surface-active compounds during HPMCs adsorption at the oil–water interface, some measurements with purified sunflower oil were done. Low levels of (or weakly surface active) compounds in the sunflower oil were present as shown in Fig. 2, with effects of up to 10 mN/m. It can be noticed that oil impurities adsorb rapidly and reach an equilibrium value at very short times (i.e. <2000 s). This behaviour is characteristic of low molecular weight surfactants. Surface-active components in sunflower oil may be a mixture of monoglycerides, free fatty acids and phospholipids. According to Wüstneck et al. (1999) such contaminants may be even essential for the interfacial behaviour of oil. Nevertheless, the removal of impurities did not significantly affect the interfacial tension evolution in the presence of HPMC (Fig. 2). Murray (1997) also claimed that the oil compounds present, do not generated substantial differences when studying the adsorption of bovine serum albumin (BSA) at the oil–water interface so no special precautions were taken to remove these compounds.

In a recent work (Camino, Perez, Carrera Sanchez, Rodriguez Patino, & Pilosof, 2009), we have demonstrated that only at HPMC concentrations lower than 10^{-5}%wt, the surface pressure values are affected by oil surface-active compounds. At such low concentrations this effect can be magnified (Williams & Prins, 1996).

In the same work, we stayed that HPMC at concentrations above 10^{-5}%wt displaced the low levels of impurities present, as shown by the high equilibrium surface pressure values reached at 10^{-5}%wt by all the polysaccharides (around 20 mN/m), which remained almost constant when increasing HPMC bulk concentration. HPMC and impurities may compete for the interface, but HPMC dominates the surface pressure even at short adsorption times (Camino, Perez, Carrera Sanchez, et al., 2009).

Table 2
Zeta potential (mV) of HPMC solutions.

HPMC	pH3[a]	pH6[a]
E4M	−1.04 ± 0.10	+0.81 ± 0.08
E50LV	−1.22 ± 0.15	+ 0.79 ± 0.10
E15LV	−1.23 ± 0.08	+0.41 ± 0.15
E5LV	−1.81 ± 0.05	+0.78 ± 0.05

[a] Mean ± SD of at least $n = 2$.

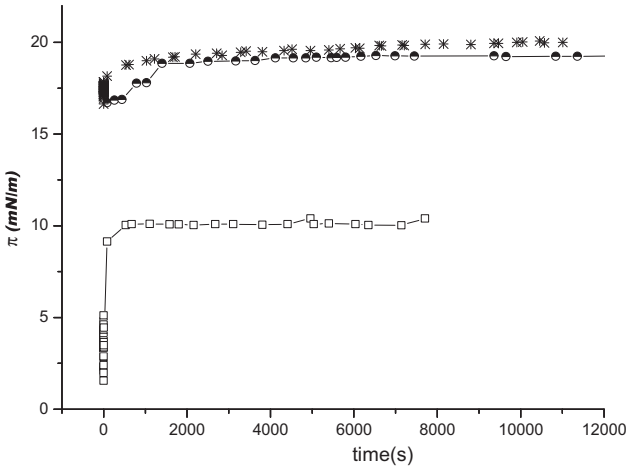

Fig. 2. Time-dependent surface pressure for commercial sunflower oil-buffer (with no added HPMC), (□), and E5LV 1%wt bulk concentration at the commercial sunflower oil–water, (*) and purified sunflower oil–water (◑) interface. Temperature 20 °C, pH6.0 and $I = 0.05$ M.

Fig. 3 shows the evolution of surface pressure as a function of adsorption time for 1×10^{-2}%wt (Fig. 3A), 1%wt (Fig. 3B) and 2%wt (Fig. 3C) HPMCs bulk concentrations at pH6.

At 1×10^{-2}%wt bulk concentration and $t < 8000$ s (Fig. 3A), the increase in surface pressure followed the order E4M > E15LV ≅ E5LV > E50LV and only E4M seems to get a steady-state π value. The higher E4M surface activity evolution at this concentration should be related to its molecular structure. E4M posses the lower number of methyl (hydrophobic) substituents but as was previously pointed out (Nahringbauer, 1995; Pérez et al., 2007; Wollenweber et al., 2000) the surface tension decrease is not dependent on the molar adsorption of the polymer, but it depends on the number of polymer segments, which are in actual contact with the surface. This means that the surface properties of a polymer depend on the length and distribution of trains, loops and tails. The average degree of polymerization of E4M is four times higher than the others (data supplied by Dow Chemical Co.), which involves an increase in the number of segments that potentially could be adsorbed per mol of polymer (Perez et al., 2006). After 8000 s, the π–t curves for E5LV, E50LV and specially E15LV continued to increase. This fact would obey to the higher number of hydrophobic groups (methyl) that these three polysaccharide posses in comparison with E4M and their lower molecular weight (Table 1).

At 1%wt bulk concentration (Fig. 3B) E5LV showed the higher surface activity and E4M seemed to get a pseudo steady-state value as was previously discussed. E15LV and E50LV showed a continuous increment in surface pressure indicating a continuous adsorption and rearrangement at this interface. Nevertheless, for all the HPMCs it was observed an increase of surface pressure with increasing concentration from 10^{-2}% to 1%.

E5LV possessing the higher % methyl groups and the low molecular weight (Table 1), would allow a higher surface pressure increment, followed by E15LV and E50LV. Baeza, Carrera Sanchez, Pilosof, and Rodríguez Patino (2004) also found a correlation between the higher increase in surface pressure and the higher degree of esterification and viscosity of propilenglicol alginates (PGA) at the air–water interface.

At 2% bulk concentration (Fig. 3C) very small differences between all HPMCs surface pressure were observed. The surface pressure values reached were similar to that at 1% bulk concentration (Fig. 3B). The fact that the increase in HPMC concentration in the bulk phase from 1%wt to 2%wt does not cause a significant

increment in surface pressure should be associated to interface saturation (Baeza, Carrera Sanchez, et al., 2004). Nevertheless, E5LV showed a significant decrease in surface pressure at 2%wt, probably due to a higher self-assembly in the bulk at this concentration (data not shown).

Fig. 4 shows the evolution of surface pressure as a function of adsorption time for 1×10^{-2}% (Fig. 4A), 1% (Fig. 4B) and 2%wt (Fig. 4C) HPMCs bulk concentrations at pH3. As for pH6, no lag time was observed in the π–t curves. It is interesting to remark that for the three bulk concentrations studied, the surface pressure of all HPMCs reached lower values than at pH6.

The lowest molecular weight HPMC, E5LV, showed the highest surface pressure at all the concentrations. This polysaccharide, with the higher % of methyl groups and the lower molecular weight (Table 1), would rapidly adsorb and easily interact with hydrogen carbon chains of oil.

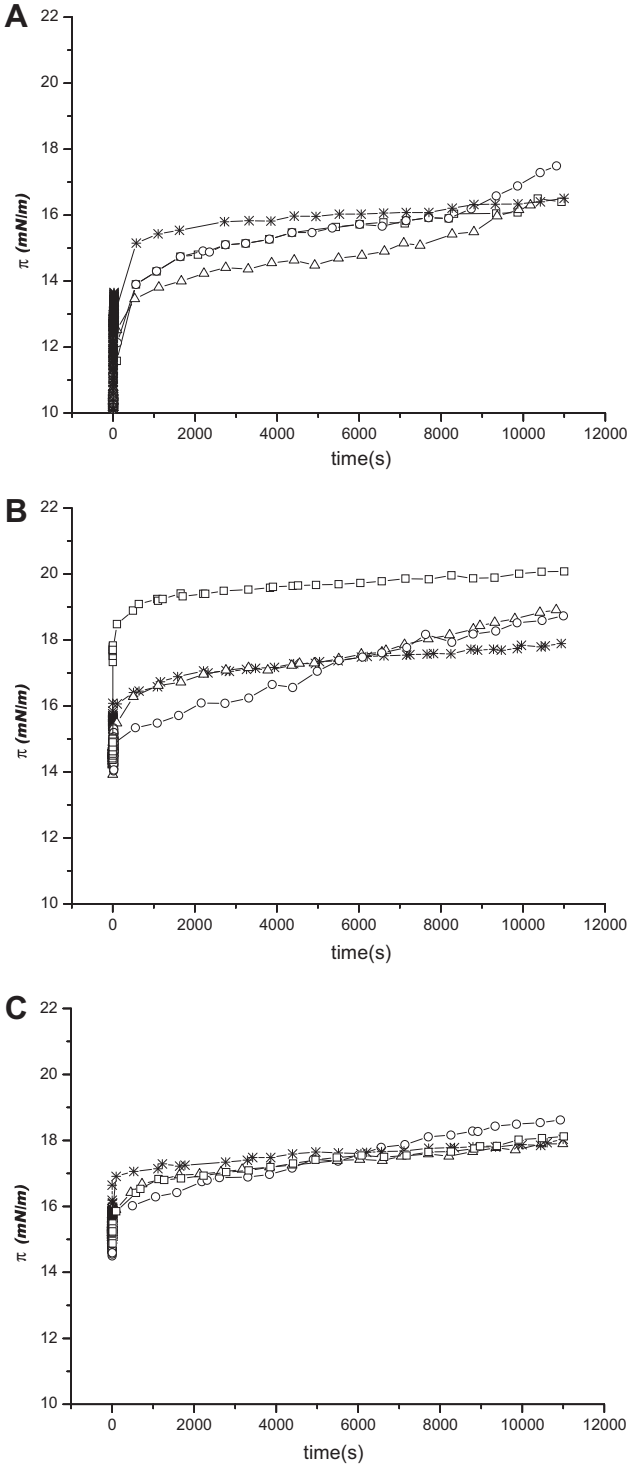

Fig. 3. Time-dependent surface pressure for E4M (*), E50LV (△), E15LV (○) and E5LV (□) adsorbed films at the oil–water interface at pH6 for 1×10^{-2}%wt (A), 1%wt (B) and 2%wt (C) concentration of HPMC in the bulk phase. Temperature 20 °C and $I = 0.05$ M.

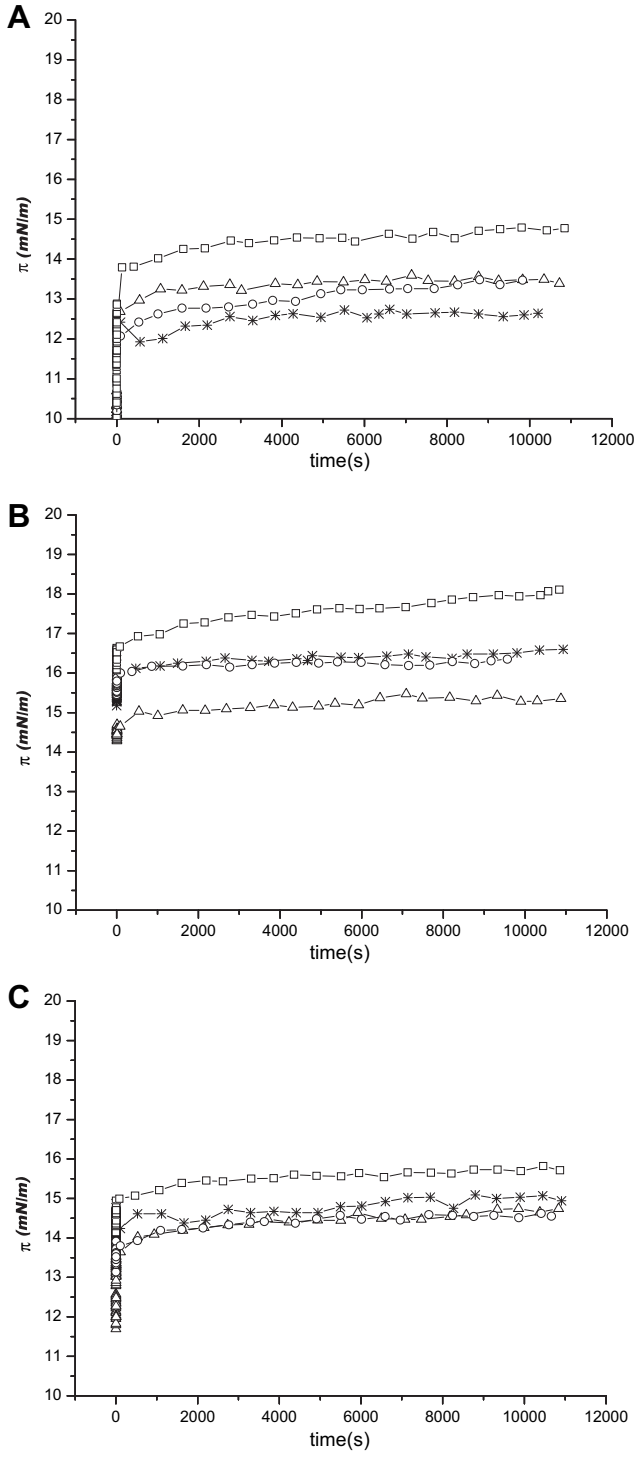

Fig. 4. Time-dependent surface pressure for E4M (*), E50LV (△), E15LV (○) and E5LV (□) adsorbed films at the oil–water interface at pH3 for 1×10^{-2}%wt (A), 1%wt (B) and 2%wt (C) concentration of HPMC in the bulk phase. Temperature 20 °C and $I = 0.05$ M.

3.3. Kinetics of HPMCs adsorption at the oil–water interface

The kinetics of adsorption at the oil–water interface can be monitored by measuring changes in surface pressure (π) with time. As the rate of surface pressure change depends primarily on the rate of adsorption, Ward & Tordai equation (equation (1)) was used to describe these changes upon time. If the diffusion of the HPMCs at the O/W interface controls the adsorption process, a plot of π–$t^{1/2}$ will then be linear (de Feijter & Benjamins, 1987; MacRitchie, 1990; Xu & Damodaran, 1994) and the slope of this plot will be the diffusion rate constant.

At higher adsorption time, after the very short period controlled by diffusion, an energy barrier for HPMC adsorption appears, which can be attributed to adsorption, penetration, unfolding, and rearrangements of the polysaccharide at the interface.

It was found that the diffusion step for these polysaccharides at pH6 (except for HPMCs 10^{-2}%wt) was too fast ($\pi > 10$ mN/m), to be detected by the experimental technique used in this work, as deduced from the π–$t^{1/2}$ plots (data not shown).

At 10^{-2}%wt HPMCs bulk concentration the rate of diffusion of E4M was the lowest (Table 3) in agreement with its higher molecular weight that would retard the diffusion step. Nevertheless, the presence of surface-active compounds from the oil phase could compete with HPMC for the interface and could affect the observed diffusion rates.

After an initial diffusion of HPMCs at both interfaces, the rate of HPMCs adsorption is controlled by the penetration and rearrangement of the macromolecules at the interfaces (Pérez et al., 2008; Rodríguez Niño & Rodríguez Patino, 2002). Malmsten and Lindman (1990) working with EHEC found that the adsorbed amount increases immediately after addition of the polymer solution, after which it levels off indicating the interface saturation.

In practice, a plot of equation (2) usually yields two or more linear regions (data not shown). The initial slope is taken as a first-order rate constant of penetration (Kads), while the second slope is taken as a first-order rate constant of molecular rearrangement (Kreor), occurring among a more or less constant number of adsorbed molecules. The fit of the experimental data to the mechanism was made at a time interval based on the best linear regression coefficient. However, because biopolymer adsorption at fluid interfaces is very time-consuming, no attempt was made to discuss the experimental data for the second rearrangement step of previously adsorbed protein molecules.

Table 3 summarizes the rates of adsorption for the HPMCs studied. The K_{ads} are in the same order of magnitude for all the HPMCs, being slightly higher for 1%wt. Multilayer formation of collapsed interfacial monolayer would slow down Kads at 2%wt (Pérez et al., 2008).

The higher Kads for E4M would be related with its higher number of potential adsorbing groups along the molecule backbone and with no cluster formation, being predominant the monomeric form. Similar results were obtained by Pérez et al., (2008) when studying the HPMCs adsorption at the A/W interface.

Table 4 summarizes the rate of diffusion and adsorption at pH3 for the three concentrations studied.

The rate of diffusion at 10^{-2}% HPMC was lower for E50LV and E4M which had the higher molecular weight (Table 1). At this pH, all the K_{diff} are higher than that obtained at pH6, probably related to the lower cluster formation tendency at pH3 (Fig. 1). As for pH6, at 10^{-2}%wt the presence of surface-active compounds from the oil phase, could compete with the HPMCs for the interface.

The rate of adsorption, Kads, was higher at 10^{-2}%wt bulk concentration, mainly for E4M and E50LV. At higher polysaccharide concentration, an energy barrier exists to adsorption and, in consequence, the ability of the HPMC molecule to create space in the existing film and penetrate and rearrange at the interface is rate-determining. Moreover, the conformational change present at pH3 (Table 2) would also impede the new arriving molecules to adsorb.

3.4. Viscoelastic characteristic of HPMCs films at the oil–water interface

The time evolution of surface dilatational elasticity (E_d) and loss angle tangent ($\tan\delta$) for HPMCs adsorbed films were obtained simultaneously during the study of the dynamics of film formation.

Fig. 5 shows the time-dependent evolution of surface dilatational elasticity (E_d) at pH6 for 10^{-2}%wt (Fig. 5A), 1%wt (Fig. 5B) and 2%wt (Fig. 5C) HPMC bulk concentration. At all concentrations all the HPMCs presented a continuous increase in E_d values indicating a slow and a gradual evolution of interfacial structure. The slow film structure evolution is also revealed by the evolution of the relative viscoelasticity of films ($\tan\delta$) in Fig. 6. The hydrophobic interactions between HPMC molecules necessary to form an elastic film would be restricted by solvation of the hydrophobic groups in the oil phase (Camino, Perez, & Pilosof, 2009).

Generally, E15LV and E5LV showed the best ability to form elastic films and E4M the lowest, which could be attributed to their higher methyl substitution which causes a strong hydrophobic interaction. As shown in Fig. 1, E5LV and E15LV exhibited a strong tendency to cluster formation at pH6.

Time dependence of relative viscoelasticity ($\tan\delta$) for HPMCs films shown in Fig. 6 indicate that viscoelastic films ($\tan\delta < 1$) are

Table 3
Kinetic parameters for HPMCs adsorption at pH6 at the O/W interface. 20 °C and $I = 0.05$ M.

HPMC (%wt)	$K_{diff} \times 10^{4a}$ (m/Nm $s^{0.5}$) (LR)	$K_{ads} \times 10^{4a}$ (s^{-1}) (LR)	$t_{end\ ads}$ (s)
E4M 10^{-2}	7.00 ± 0.10 (0.97)	1.62 ± 0.11 (0.97)	8000
E4M 1	–	2.10 ± 0.06 (0.99)	8500
E4M 2	–	1.85 ± 0,06 (0,98)	>10,000
E50LV 10^{-2}	6.30 ± 0.06 (0.97)	1.09 ± 0.09 (0.96)	8000
E50LV 1	–	1.78 ± 0.08 (0.97)	8800
E50LV 2	–	1.73 ± 0.11 (0.98)	>10,000
E15LV 10^{-2}	11.14 ± 0.09 (0.98)	1.39 ± 0.17 (0.89)	7200
E15LV 1	–	2.01 ± 0.17 (0.97)	7400
E15LV 2	–	1.77 ± 0.14 (0.97)	8000
E5LV 10^{-2}	10.82 ± 0.05 (0.98)	1.14 ± 0.09 (0.98)	6800
E5LV 1	–	1.88 ± 0.07 (0.99)	6900
E5LV 2	–	1.60 ± 0.08 (0.98)	8000

K_{diff}, K_{ads}: rate constant of diffusion, penetration/adsorption respectively.
LR: linear regression coefficient.
[a] Mean ± SD of at least $n = 2$.

Table 4
Kinetic parameters for HPMCs adsorption at pH3 at the O/W interface. 20 °C and $I = 0.05$ M.

HPMC (%wt)	$K_{diff} \times 10^{4a}$ (m/Nm $s^{0.5}$) (LR)	$K_{ads} \times 10^{4a}$ (s^{-1}) (LR)	$t_{end\ ads}$ (s)
E4M 10^{-2}	8.17 ± 0.08 (0.97)	3.49 ± 0.48 (0.92)	>10,000
E4M 1	–	1.24 ± 0.21 (0.85)	>10,000
E4M 2	–	1.72 ± 0.55 (0.82)	>10,000
E50LV 10^{-2}	7.95 ± 0.15 (0.96)	11.1 ± 1.34 (0.94)	>10,000
E50LV 1	–	1.97 ± 0.43 (0.98)	>10,000
E50LV 2	–	1.95 ± 0.27 (0.95)	>10,000
E15LV 10^{-2}	25.68 ± 0.05 (0.99)	2.66 ± 0.23 (0.96)	>10,000
E15LV 1	–	2.4 ± 0.39 (0.92)	>10,000
E15LV 2	–	1.98 ± 0.22(0.91)	>10,000
E5LV 10^{-2}	38.72 ± 0.05 (0.98)	1.56 ± 0.08(0.98)	5800
E5LV 1	–	1.55 ± 0.10(0.97)	5800
E5LV 2	–	1.57 ± 0.11(0.95)	6000

K_{diff}, K_{ads}: rate constant of diffusion and penetration/adsorption respectively.
LR: linear regression coefficient.
[a] Mean ± SD of at least $n = 2$.

formed in most cases. tan δ values well below 1, reached upon adsorption, indicated that the films had a gel-like structure, which involved the association of the hydrophobic methyl groups of HPMC (Kita, Kaku, Kubota, & Dobashi, 1999). For E50LV 10^{-2}%wt and E4M 2%wt, a viscoelastic film was formed only at long term adsorption (8000 s).

Fig. 7 shows the time-dependent evolution of surface dilatational elasticity (E_d) for 10^{-2}%wt (Fig. 7A), 1%wt (Fig. 7B) and 2%wt (Fig. 7C) bulk concentration at pH3.

The continuous increase of the elastic character was not evident at this pH as it was shown at pH6. The values of Ed were very low (<5 mN/m) for all the concentrations studied and did not change

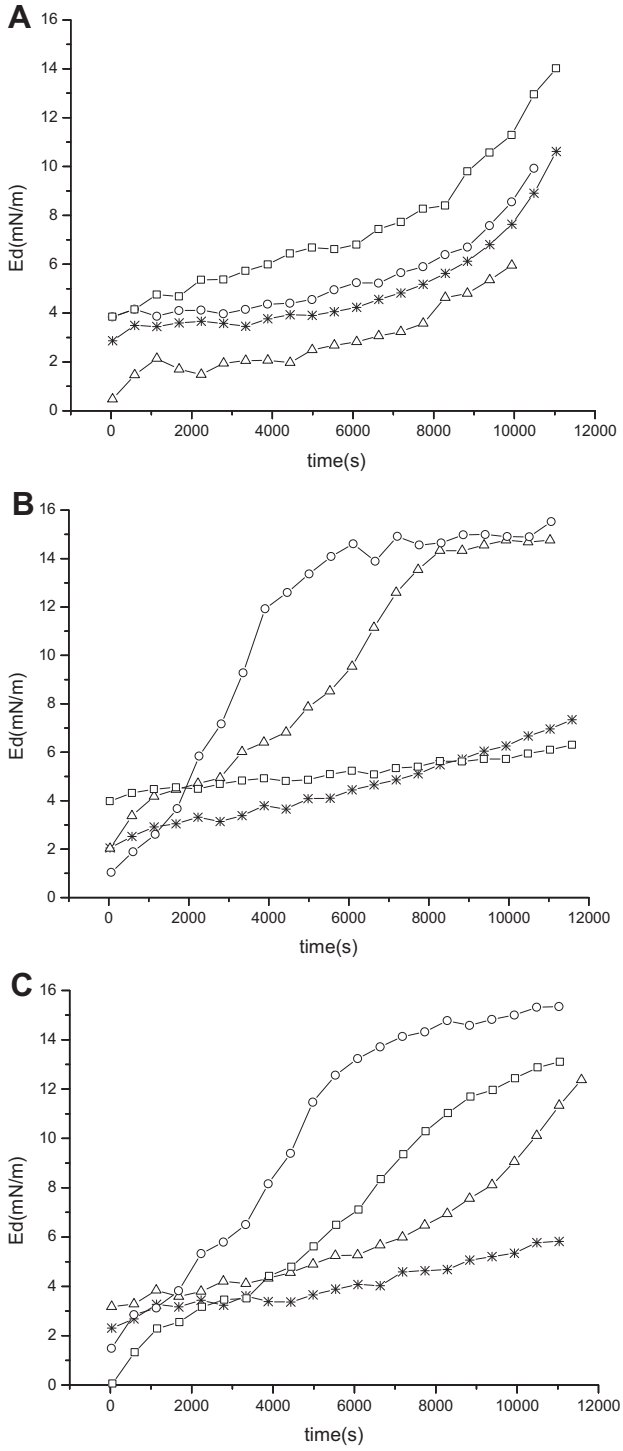

Fig. 5. Time-dependent surface dilatational elasticity, E_d, for E4M (*), E50LV (△), E15LV (○) and E5LV (□) adsorbed films at the oil–water interface at pH6 for 1×10^{-2}%wt (A), 1%wt (B) and 2%wt (C) concentration of HPMC in the bulk phase. Temperature 20 °C and $I = 0.05$ M.

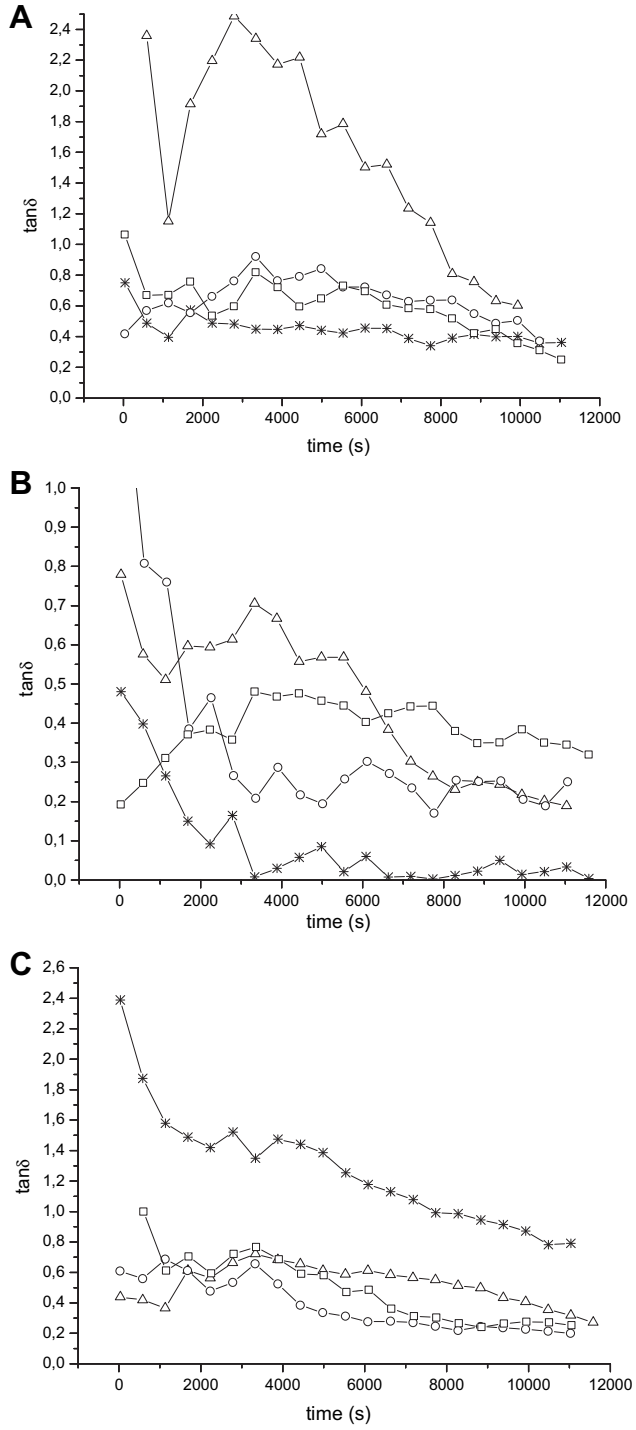

Fig. 6. Time-dependent phase angle tangent, tan δ, for E4M (*), E50LV (△), E15LV (○) and E5LV (□) adsorbed films at the oil–water interface at pH6 for 1×10^{-2}%wt (A), 1% wt (B) and 2%wt (C) concentration of HPMC in the bulk phase. Temperature 20 °C and $I = 0.05$ M.

with adsorption time, except for E4M 2%wt (insert Fig. 7C) where Ed values decreased with time up to 15 mN/m, and seemed to level off. When analysing tan δ (not shown), only HPMCs at 1%wt and particularly E5LV formed viscoelastic films (tan $\delta < 1$) at all times. At 2%wt none of the HPMCs formed viscoelastic films and at 10^{-2}%, only E5LV presented tan $\delta < 1$ at $t < 6000$ s. The low ability to form elastic films at pH3 is related to the low tendency of HPMCs to associate at this pH as seen in the bulk by DLS (Fig. 1).

The evolution of surface dilatational modulus (E) with surface pressure for the adsorption of HPMCs is shown in Fig. 8A for pH3 and in Fig. 8B for pH6. If the surface dilatational modulus is only due to the amount of HPMC adsorbed at the interfaces, all E data should be normalized in a single master curve. Fig. 8 shows that this normalization was not possible for any bulk concentration, indicating a non-ideal behaviour and reflecting the impact of macromolecule interactions.

As for other biopolymers, like proteins (Horne & Rodriguez Patino, 2003; Rodríguez Patino, Molina, Carrera, Rodríguez Niño, & Añon, 2003) and polysaccharides (Baeza, Sanchez, Pilosof, & Patino, 2004), at pH6 E increased with interfacial pressure and this dependence reflects the existence of higher interactions within the adsorbed polysaccharide residues.

Nevertheless, the surface dilatational modulus of HPMCs films at pH3 (Fig. 8A) were very small and did not increase with interfacial pressure, revealing the absence of interactions within the adsorbed HPMCs residues at this pH.

4. Discussion

As it was previously reported, the self-assembly of HPMC in solution is driven by hydrophobic interactions between the hydrophobic substituents, mainly methyl groups (Funami et al., 2007; Kato et al., 1978; Sarkar & Walker, 1995).

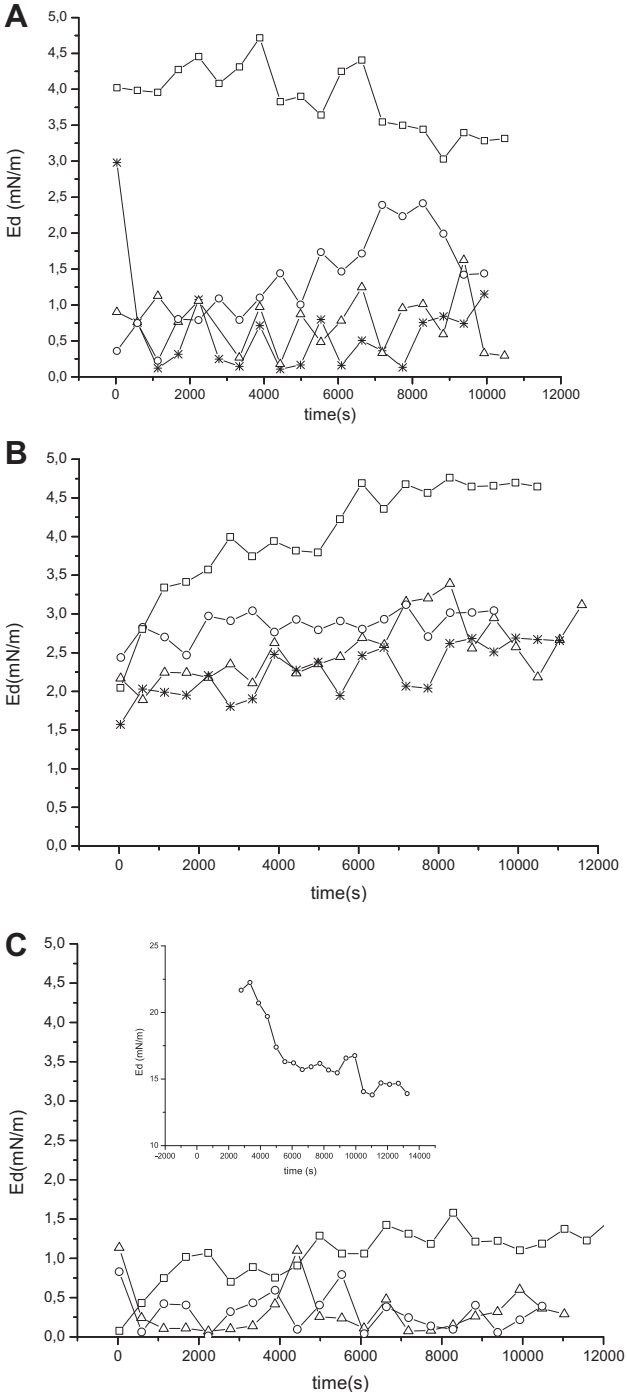

Fig. 7. Time-dependent surface dilatational elasticity, E_d, for E4M (*), E50LV (△), E15LV (○) and E5LV (□) adsorbed films at the oil–water interface at pH3 for 1×10^{-2}%wt (A), 1%wt (B) and 2%wt (C) concentration of HPMC in the bulk phase. Temperature 20 °C and $I = 0.05$ M.

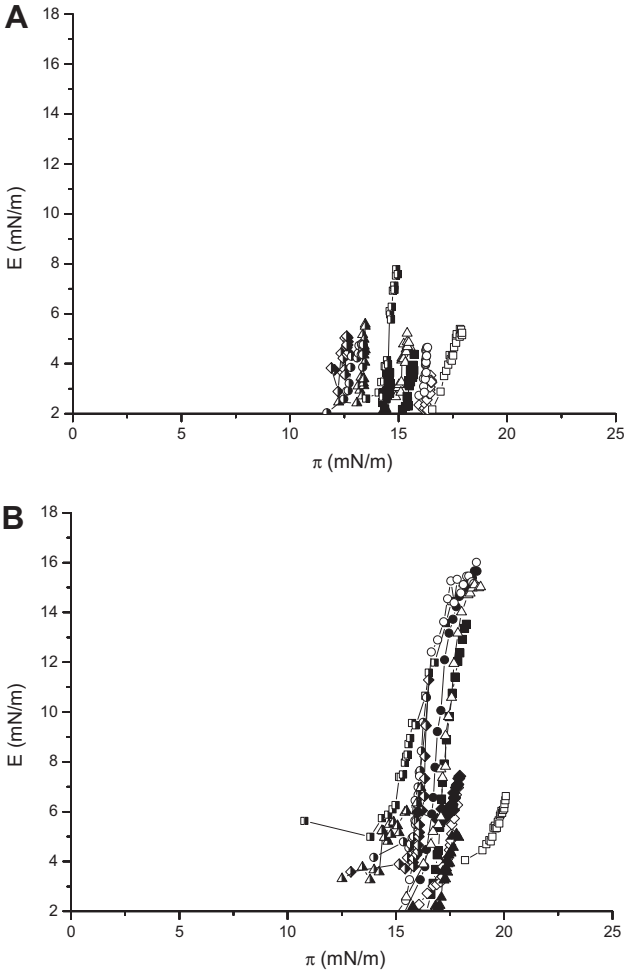

Fig. 8. Surface dilatational modulus, E, as a function of surface pressure for HPMCs adsorbed films at the oil–water interface at pH3 (A) and pH6 (B). Frequency: 0.1 HZ. Amplitude of compression/expansion cycle: 10%. HPMC concentration in the drop bulk phase: 1×10^{-2}%wt (E4M, E50LV, E15LV, ◑; E5LV), 1%wt (E4M, ◇; E50LV, △; E15LV, ○; E5LV, □) and 2%wt (E4M, ◆; E50LV, ▲; E15LV, ●; E5LV, ■). Temperature 20 °C and $I = 0.05$ M.

Other polysaccharides also tend to form clusters in solution. Rouzes, Durand, Leonard, and Dellacherie (2002) claimed that hydrophobically modified dextrans behaved like classical associative polymers in aqueous solution forming compact aggregates. For dextrans with lower substitution ratios, aggregation occurs at higher concentrations.

Henni et al. (2005) reported that physicochemical characteristics of hydrophobically modified carboxymethylpullulan derivates are related to both intra and/or intermolecular associations between their hydrophobic segments in aqueous solution, which would lead to the formation of more or less aggregated structures containing hydrophobic microdomains.

Sun et al. (2007) reported that hydrophobically modified hydroxyethyl cellulose (HMHEC) presented much better thickening ability than low molecular weight surfactants due to the association of hydrophobic groups in the backbone. As the concentration increased, the viscosity increased because of association of the hydrophobic groups which leads to formation of a transient three-dimensional network. As for HPMC, if the hydrophobicity and molecular weight increases, the intermolecular association starts at lower concentrations because the hydrophobic groups are closer.

The results of present work have shown that the behaviour of HPMCs in solution and at the oil–water interface reveals a significant effect of pH, indicating that pH has a strong impact on the occurrence of hydrophobic interactions among HPMC molecules.

Tritt-Goc and Pislewski (2002) studying HPMC hydration at pH2 and pH6, found that at lower pH predominate a higher number of hydrogen bonds between the protons of the solvent and the HPMCs molecules. Because of the interactions of the molecules with the surrounding medium, the hydrophobic interactions (responsible of aggregate formation) would be impeded at pH3. This would be the reason why at lower pHs, a predominant HPMC monomeric form is found in solution.

Sawyer and Reed (2001) also pointed out that the change in pH influences the properties of the HPMCs molecules when adsorbing at solid particles. They observed the hydrogen bonding to be pH dependent, with reduced adsorption to the solid interface at higher pHs, indicating a higher interaction between HPMCs molecules and not with the solid particle.

Another explanation of the predominance of the monomeric form found at pH3 and the low degree of association at the interface is based on the conformational change. As discussed previously, the presence of chlorine ions in the solutions would interact with the *cage-like* structures impeding the hydrophobic interactions.

The surface behaviour was strongly influenced by pH and kept correlation with DLS results. The dynamic surface pressure as well as the rate of adsorption/penetration were lower at pH3. At this pH, an electrostatic repulsion is present due to a net negative charge. The molecules arriving to the interface from the bulk would be impeded their adsorption and rearrangement due to the presence of the charge of previously adsorbed molecules. Moreover, in most cases the formation of a viscoelastic film was prevented.

Pérez et al. (2008) related the surface pressure increment and the continuous increase of E_d for HPMCs at the air–water interface with higher interactions and reorganization of the hydrophobic groups previously adsorbed.

In conclusion, the pH-modulated hydrophobic interactions between HPMC molecules have shown to impact strongly their performance in the bulk and at the oil–water interface. Among all the HPMC studied, E5LV showed over all the best performance at the oil–water interface due to its low molecular weight which allows a fast diffusion to the interface and a high decrease of interfacial tension. Moreover, its high hydrophobicity allows a strong tendency to interact at the interface to form elastic films.

Acknowledgements

This research was supported by CYTED through project 105PI0274. The authors also acknowledge the support from CYCYT through grant AGL2007-60045, Junta de Andalucía through grant PO6-AGR-01535, , and Universidad de Buenos Aires, Agencia Nacional de Promoción Científica y Tecnológica and Consejo Nacional de Investigaciones Científicas y Técnicas de la República Argentina.

References

Akiyama, E., Kashimoto, A., Fukuda, K., Hotta, H., Suzuki, T., & Kitsuki, T. (2005). Thickening properties and emulsification mechanisms of new derivatives of polysaccharides in aqueous solution. *Journal of Colloid and Interface Science, 282* (2), 448–457.

Arboleya, J.-C., & Wilde, P. J. (2005). Competitive adsorption of proteins with methylcellulose and hydroxypropyl methylcellulose. *Food Hydrocolloids, 19*(3), 485–491.

Baeza, R., Carrera Sanchez, C., Pilosof, A. M. R., & Rodríguez Patino, J. M. (2004). Interactions of polysaccharides with [beta]-lactoglobulin spread monolayers at the air–water interface. *Food Hydrocolloids, 18*(6), 959–966.

Baeza, R., Carrera Sanchez, C., Pilosof, A. M. R., & Rodríguez Patino, J. M. (2005). Interactions of polysaccharides with [beta]-lactoglobulin adsorbed films at the air–water interface. *Food Hydrocolloids, 19*(2), 239–248.

Baeza, R., Sanchez, C. C., Pilosof, A. M. R., & Patino, J. M. R. (2004). Interfacial and foaming properties of prolylenglycol alginates: effect of degree of esterification and molecular weight. *Colloids and Surfaces B: Biointerfaces, 36*(3–4), 139–145.

Camino, N. A., Perez, O. E., Carrera Sanchez, C., Rodriguez Patino, J. M., & Pilosof, A. M. R. (2009). Hydroxypropylmethylcellulose surface activity at equilibrium and adsorption dynamics at the air–water and oil–water interfaces. *Food Hydrocolloids, 23*, 2359–2368.

Camino, N. A., Perez, O. E., & Pilosof, A. M. R. (2009). Modification of hydroxypropylmethylcellulose by high intensity ultrasound. *Food Hydrocolloids, 23*, 1089–1095.

Daniels, R., & Barta, A. (1993). Preparation, characterization and stability assessment of oil-in-water emulsions with hydroxypropylmethylcellulose as emulsifier. In *Proceedings of Pharmaceutics Technology Conference* (pp. 51–60). Elsinore.

Daniels, R., & Barta, A. (1994). Pharmacopoeial cellulose ethers as oil in water emulsifiers 1. Interfacial properties. *European Journal of Pharmaceutical and Biopharmaceutical, 40*, 128–133.

de Feijter, J. A., & Benjamins, J. (1987). Adsorption kinetics of proteins at the air–-water interface. In E. Dickinson (Ed.), *Food emulsions and foams*. New York: Marcel Dekker.

Doublier, J. L., & Launay, B. (1981). Rheology of galactomannan solutions: comparative study of guar gum and locust bean gum. *Journal of Texture Studies, 12*, 151–172.

Funami, T., Kataoka, Y., Hitoe, M., Asai, I., Takahashi, R., & Nishinari, K. (2007). Thermal aggregation of methylcellulose with different molecular weights. *Food Hydrocolloids, 21*, 46–58.

Graham, D. E., & Phillips, M. C. (1979). Proteins at liquid interfaces: III. Molecular structures of adsorbed films. *Journal of Colloid and Interface Science, 70*(3), 427–439.

Henni, W., Deyme, M., Stchakovsky, M., LeCerf, D., Picton, L., & Rosilio, V. (2005). Aggregation of hydrophobically modified polysaccharides in solution and at the air–water interface. *Journal of Colloid and Interface Science, 281*, 316–324.

Horne, D. S., & Rodriguez Patino, J. M. (2003). *Biopolymers at interfaces* (pp. 857–900). New York: Marcel Dekker.

Kato, T., Yokoyama, M., & Takahashi, A. (1978). Melting temperatures of thermally reversible gels IV. *Colloid and Polymer Science, 266*, 15–21.

Kita, R., Kaku, T., Kubota, K., & Dobashi, T. (1999). Pinning of phase separation of aqueous solution of hydroxypropylmethylcellulose by gelation. *Physics Letters A, 259*, 302–307.

Labourdenne, S., Gaudry-Rolland, N., Letellier, S., Lin, M., Cagna, A., & Esposito, G. (1994). The oil-drop tensiometer: potential applications for studying the kinetics of (phospho)lipase action. *Chemistry and Physics of Lipids, 71*(2), 163–173.

Lucassen, J., & van den Temple, M. (1972). Dynamic measurements of dilatational properties of a liquid interface. *Chemical Engineering Science, 27*, 1283–1291.

MacRitchie, F. (1990). *Chemistry at interfaces*. San Diego, CA: Academic Press.

Malmsten, M., & Lindman, B. (1990). Ellipsometry studies of the adsorption of cellulose ethers. *Langmuir, 6*, 357–364.

Martinez, K., Carrera Sanchez, C., Ruiz Henestrosa, V. P., Rodriguez Patino, J. M., & Pilosof, A. M. R. (2007). Soy protein–polysaccharides interactions at the air–-water interface. *Food Hydrocolloids, 21*, 804–812.

McClements, D. J. (1999). *Food emulsions. Principles, practice and techniques*. New York: CRC Press.

Mezdour, S., Cuvelier, G., Cash, M. J., & Michon, C. (2007). Surface rheological properties of hydroxypropyl cellulose at air–water interface. *Food Hydrocolloids, 21*(5–6), 776–781.

Mezdour, S., Lepine, A., Erazo-Majewicz, P., Ducept, F., & Michon, C. (2008). Oil/water surface rheological properties of hydroxypropyl cellulose (HPC) alone and mixed with lecithin: contribution to emulsion stability. *Colloids and Surfaces A: Physicochemical and Engineering Aspects, 331*(1–2), 76–83.

Moreau, L., Kim, H.-J., Decker, E. A., & McClements, D. J. (2003). Production and characterization of oil-in-water emulsions containing droplets stabilized by β-lactoglobulin–pectin membranes. *Journal of Agricultural and Food Chemistry, 51* (22), 6612–6617.

Murray, B. S. (1997). Equilibrium and dynamic surface pressure–area measurements on protein films at air–water and oil–water interfaces. *Colloids and Surface A: Physicochemical and Engineering Aspects, 125*, 73–83.

Nahringbauer, I. (1995). Dynamic surface tension of aqueous polymer solutions, I: ethyl(hydroxyethyl)cellulose (BERMOCOLL cst-103). *Journal of Colloid and Interface Science, 176*(2), 318–328.

Ochoa Machiste, E., & Buckton, G. (1996). Dynamic surface tension studies of hydroxypropylmethylcellulose film-coating solutions. *International Journal of Pharmaceutics, 145*(1–2), 197–201.

Pérez, O. E., Carrera Sánchez, C., Pilosof, A. M. R., & Rodríguez Patino, J. M. (2009). Kinetics of adsorption of whey proteins and hydroxypropyl-methyl-cellulose mixtures at the air–water interface. *Journal of Colloid and Interface Science, 336*, 485–496.

Perez, O. E., Carrera Sanchez, C., Rodriguez Patino, J. M., & Pilosof, A. M. R. (2006). Thermodynamics and dynamics characteristics of hydroxypropylmethylcellulose adsorbed films at the air–water interface. *Biomacromolecules, 7*, 388–393.

Pérez, O. E., Carrera-Sánchez, C., Rodríguez-Patino, J. M., & Pilosof, A. M. R. (2007). Adsorption dynamics and surface activity at equilibrium of whey proteins and hydroxypropyl-methyl-cellulose mixtures at the air–water interface. *Food Hydrocolloids, 21*(5–6), 794–803.

Pérez, O. E., Sánchez, C. C., Pilosof, A. M. R., & Rodríguez Patino, J. M. (2008). Dynamics of adsorption of hydroxypropyl methylcellulose at the air–water interface. *Food Hydrocolloids, 22*(3), 387–402.

Perrin, P., & Lafuma, F. (1998). Low hydrophobically modified poly(acrylic acid) stabilizing macroemulsions: relationship between copolymer structure and emulsions properties. *Journal of Colloid and Interface Science, 197*(2), 317–326.

Rodríguez Niño, M. R., & Rodríguez Patino, J. M. (2002). Effect of the aqueous phase composition on the adsorption of bovine serum albumin to the air–water interface. *Industrial and Engineering Chemistry Research, 41*, 1489–1495.

Rodríguez Patino, J. M., Molina, S. E., Carrera, C., Rodríguez Niño, M. R., & Añon, C. (2003). Dynamic properties of soy globulin adsorbed films at the air–water interface. *Journal of Colloid and Interface Science, 268*, 50–57.

Rouzes, C., Durand, A., Leonard, M., & Dellacherie, E. (2002). Surface activity and emulsification properties of hydrophobically modified dextrans. *Journal of Colloid and Interface Science, 253*, 217–223.

Sarkar, N. (1977). Thermal gelation properties of methyl and hydroxypropylmethylcellulose. In IFT (Ed.), *Proceeding of 1977 annual meeting of the Institute of Food Technologists* (pp. 1073–1087). Philadelphia, USA.

Sarkar, N., & Walker, L. C. (1995). Hydration–dehydration properties of methylcellulose and hydroxypropylmethylcellulose. *Carbohydrate Polymers, 27*, 177–185.

Sawyer, C. B., & Reed, J. S. (2001). Adsorption of hydroxypropylmethylcellulose in an aqueous system containing multicomponent oxide particles. *Journal of American Ceramic Society, 84*(6), 1241–1249.

Sun, W., Sun, D., Wei, Y., Liu, S., & Zhang, S. (2007). Oil-in-water emulsions stabilized by hydrophobically modified hydroxyethyl cellulose: adsorption and thickening effect. *Journal of Colloid and Interface Science, 311*(1), 228–236.

Tritt-Goc, J., & Pislewski, N. (2002). Magnetic resonance imaging study of the swelling kinetics of hydroxypropylmethylcellulose (HPMC) in water. *Journal of Controlled Release, 80*, 79–86.

U.S.P., U.-N. (2008). *United States pharmacopeia*.

Viriden, A., Wittgren, B., Andersson, T., & Larsson, A. (2009). The effect of chemical heterogeneity of HPMC on polymer release from matrix tablets. *European Journal of Pharmaceutical Sciences, 36*, 392–400.

Ward, A. F. H., & Tordai, L. (1946). Time dependence of boundary tensions of solutions I. *Journal of Chemical Physics, 14*, 353–361.

Williams, A., & Prins, A. (1996). Comparison of the dilational behaviour of adsorbed milk proteins at the air–water and oil–water interfaces. *Colloids and Surfaces A: Physicochemical and Engineering Aspects, 114*, 267–275.

Wollenweber, C., Makievski, A. V., Miller, R., & Daniels, R. (2000). Adsorption of hydroxypropyl methylcellulose at the liquid/liquid interface and the effect on emulsion stability. *Colloids and Surfaces A: Physicochemical and Engineering Aspects, 172*(1–3), 91–101.

Wüstneck, R., Moser, B., & Muschiolik, G. (1999). Interfacial dilational behaviour of adsorbed [beta]-lactoglobulin layers at the different fluid interfaces. *Colloids and Surfaces B: Biointerfaces, 15*(3–4), 263–273.

Xu, S., & Damodaran, S. (1994). Kinetics of adsorption of protein at the air–water interface from a binary mixture. *Langmuir, 10*, 472–480.